



Mathematical Modeling of Water Flow for Irrigation in a Permeable Pipe of Elliptical Cross-section

A. W. Ndegwa^{1*}, M. M. Kimathi², M. N. Kinyanjui³ and I. Chepkwony⁴

¹Mathematics Department, P.O. Box 43844-00100, Kenyatta University, Nairobi, Kenya.

²Department of Pure and Applied Mathematics, P.O. Box 52428-00200, Technical University of Kenya, Nairobi, Kenya.

³Department of Pure and Applied Mathematics, P.O. Box 62000-00200, Jomo Kenyatta University of Agriculture and Technology, Nairobi, Kenya.

⁴Mathematics Department, P.O. Box 62000-00200, Jomo Kenyatta University of Agriculture and Technology, Nairobi, Kenya.

Article Information

DOI: 10.9734/BJMCS/2015/13157

Editor(s):

(1) Kai-Long Hsiao, Taiwan Shoufu University, Taiwan.

Reviewers:

(1) Mohammad Reza Safaei, Department of Mechanical Engineering, University of Malaya, Malaysia.

(2) Anonymous, University of Texas-Pan American, Edinburg, USA.

Complete Peer review History:

<http://www.sciencedomain.org/review-history.php?iid=726&id=6&aid=6661>

Original Research Article

Received: 05 August 2014

Accepted: 12 September 2014

Published: 23 October 2014

Abstract

An unsteady incompressible fully developed flow in a horizontal flexible and permeable annular pipe of elliptic cross-section under the action of gravity is studied. The solution is obtained through a homogenization method by employing a small scale separation parameter that approximates the pipe in the form of a series. The results in terms of velocity and pressure distributions and mass flow rate inside the pipe and through the pipe wall are presented and discussed. It is shown that the pipe thickness has no influence on the water flow through the pores. We also propose that for the efficient use of water for irrigation, the elliptical pipe should be laid in a vertical position.

Keywords: Elliptical cross-section, Mass flow rate, Permeability, Fully developed flow, Scale separation, Homogenization

2010 Mathematics Subject Classification: 53C25; 83C05; 57N16

*Corresponding author: E-mail: ndegwa.ambrose@ku.ac.ke

Nomenclature

a	semi-minor axis
A	constant
b	semi-major axis
B	constant
C	constant
Da	Darcy's number
$\mathbf{e}_{x_1}, \mathbf{e}_{x_2}$	unit vectors
h	water level reservoir
H	pipe outer radius
K^*	pipe wall permeability
L^*	pipe length
p	pressure inside the pipe
P_{in}	inlet pressure
p_m	pressure in the pipe wall
q	discharge
Q	mass flow rate
Re	Reynolds number
S^*	wall thickness
\mathbf{U}	water velocity through pipe wall
\mathbf{V}	water velocity in the pipe
x	variable
x_1	pipe lateral axis
x_2	pipe longitudinal axis
x_3	pipe vertical axis
y	variable
Y^*	width of cross section less the thickness

Greek symbols

ε	$\frac{Y^*}{L^*}$ (scale separation parameter)
ϕ	pipe wall porosity
α	angle measured from the positive major axis
μ^*	water viscosity
χ	ratio between characteristic pressures
Υ	constant
ρ^*	water density
τ	dummy variable

Subscripts

res	reservoir
c	characteristic quantity
in	inlet
m	pipe wall

1 Introduction

Flow through ducts plays a very important role in irrigation, chemical, mechanical and biological engineering. These ducts are used as parts of pipe line , heat exchangers, cooling systems, chemical

reactors, gas turbines, centrifugal pumps. In this study we consider an irrigation pipe system of elliptic cross section made of a permeable and flexible material, for example canvas hoses laid on the ground and connected to an elevated reservoir so that the driving pressure is provided by gravity. The reservoir has sufficient water capacity of the order of $1m^3$. The water from the reservoir is delivered to the plants by letting it filtrate through the porous duct laid down on the ground. The end of the pipe is sealed so that the flow takes place in the dead end configuration. The key point in this irrigation system is not only to regulate the total discharge, but also to ensure that the flow rate at the pipe inlet will be the same as the total flow rate at the pipe outlets (i.e. the total flow rate through the pores)[1]. For this study we consider an incompressible viscous fluid. The fluid flow is unsteady, laminar and fully developed through a pipe of elliptical cross section.

1.1 Elliptical cross-section

[2] obtained the solution of the Navier-Stoke's equations by the lubrication approximation, that is, they assumed that the fluid flow at each axial location x along the channel resembles the fully developed flow that would exist at that location if the channel shape did not vary with x . Although the asymptotic solution method gave more accurate results compared to the lubrication approximation, the final solution for pressure drop and velocity field had a complex form even for simple cross-sectional geometries. [3] proposed a general model that accounts for gradual variations in the cross-section of microchannels and relates the pressure drop to geometrical parameters of the cross section. It's accuracy was assessed by comparing the results against experimental and numerical data for a wide variety of cross-sectional shapes. [4] used a point matching technique to calculate closed form solutions for the velocity distributions in channels of various cross sections. The approach was based on using general solution Poisson's equation in the form of trigonometric series expansion. Pressure drop and Poiseuille numbers were determined for a variety of cross sections. [5] considered flow in rectangular ducts and employed a linear stability theory to a steady laminar solution and an eigenvalue problem was generated in the matrix form. The critical Reynolds numbers were evaluated for some aspect ratios to describe the neutral curves. The study of unsteady flow of an incompressible second grade fluid in an infinitely long tube of elliptical cross-section was carried out by [6] and the resulting governing equation was solved using the separation of variables method. They showed the effect of the applied pressure gradient and an exact solution was obtained. [7] considered the laminar flow in a sharp edged tube emerging from a large reservoir. The problem was numerically simulated by solving the full elliptic Navier-Stoke's equations and using a plenum upstream of the inlet. They were able to calculate the velocity profile at the tube inlet instead of postulation. In order to study flow in elliptical pipes exhaustively, it is important to look at turbulent flow. [8] computed the turbulent flow in a pipe with elliptical cross section using a finite difference method designed to solve the Navier-Stoke's equations in orthogonal coordinates. It was shown that the flow characteristics in the pipe's cross section along the minor axis were similar to those of the turbulent flow in a plane channel.

1.2 Mass flow rate

Studies have also been carried out for mass flow rate. A three-dimensional mathematical model for the fluid flow in elliptic cylindrical pipe was presented by [9]. In their study they found that the pressure drop in elliptical cylindrical pipes is higher than in circular pipes for the same mass flow rate. [10] calculated the mass flow rate through a tube with elliptical cross-section over the whole range of the rarefaction parameter varying from the molecular regime to the hydrodynamic one. Various aspect ratios were considered. The analysis of the numerical data shows the significant influence of this aspect ratio on the mass flow rate. [11] solved the Navier-Stokes equations exactly for flow between coaxial circular cylinders and flow in an equilateral triangular pipe. The velocity fields and total flow rates were found analytically. He found that a relatively small slip length can lead to a large

increase in the total rate of fluid flow. The numerical investigation of the rarefied Poiseuille flow in the channels of elliptical and rectangular cross-sections was carried out by [12] using a second-order difference scheme. They showed that the reduced gas flow rate through a rectangular channel is greater than that through a circular or an elliptical channel. [4] showed that the pressure drop is a function of the mass flow rate and dimensions of the cross-section. They also noted that the selection of the characteristic length does not affect the calculated pressure drop.

The purpose of this work is to develop an approximate method to determine the best physical orientation of a pipe with elliptical cross-section for efficient use of piped water for irrigation by extending the previous model of [1] to a permeable pipe of elliptical cross-section. The current study presents the solution of the Navier-Stokes equations together with Darcy's Law in the rectangular coordinate system. In our study we have employed the homogenization method which eliminates the difficulties related to the explicit determination of a solution of the problem at the microscale and offering a less detailed description in the macroscale, but one which is applicable to much more complex systems [13]. [14] showed that upscaling can be usually achieved only approximately, and the result may depend on the particular upscaling scheme adopted. For the mass flow rate, a rectangular cross-section is cut out of the elliptical pipe (see figure 1) and through its variation with the angle α across the cross-section, a solution is obtained.

2 Methodology

We seek a solution for unsteady laminar fully developed flow of a Newtonian fluid with constant properties in a uniform, flexible and permeable pipe of elliptical cross-section. Finding an exact solution for such a problem is highly unlikely, but approximations can be obtained in the form of a series in terms of a small scale separation parameter, ε . The idea is to take advantage of the fact that variation in the direction of flow, x is gradual compared to variation in the orthogonal direction, y [2].

In our model, it is assumed that the length Y^* in figure (1) is small compared to the length of the pipe L^* . This separation condition is directly connected to the scale separation parameter ε , that must be small for a macroscopic equivalent model to exist [15]:

$$\varepsilon = \frac{Y^*(\text{vertical length})}{L^*(\text{horizontal length})} \ll 1$$

Looking at figure (2), the elliptical cross section has semi-major axis b and semi-minor axis a . From [12] it was noted that $\frac{b}{a} > 1$ gave an error of the order of 1% for the calculations of the flow rate. That is $a < b$. The porosity and the permeability of the wall will be denoted by ϕ and K^* respectively. The spatial coordinates are: $x^* \in (0, L^*)$, and $y^* \in (0, H^*)$, where $H^* = Y^* + S^*$, is the width of the cross-section in Fig. (3.1) and $Y^* = a \sin \alpha + (1 - \sin \alpha)b$; $\alpha \in [0, \frac{\pi}{2}]$ is the width of the cross section minus the pipe thickness with α being the angle measured from the positive major axis.

In our study we let $a = \frac{1}{2}b$ then from $Y^* = a \sin \alpha + (1 - \sin \alpha)b$ we have for $\alpha = \frac{\pi}{2}$, $Y^* = a$ and for $\alpha = 0$, $Y^* = b$

Therefore we define $\max(Y^*) = b$

This implies that

$$H^* = Y^* + S^* = a + S^*$$

The water velocity \mathbf{V}^* and the velocity \mathbf{U}^* through the porous wall can be written in terms of their components as

$$\mathbf{V}^* = V_{x_2}^* \mathbf{e}_{x_2} + V_{x_3}^* \mathbf{e}_{x_3}$$

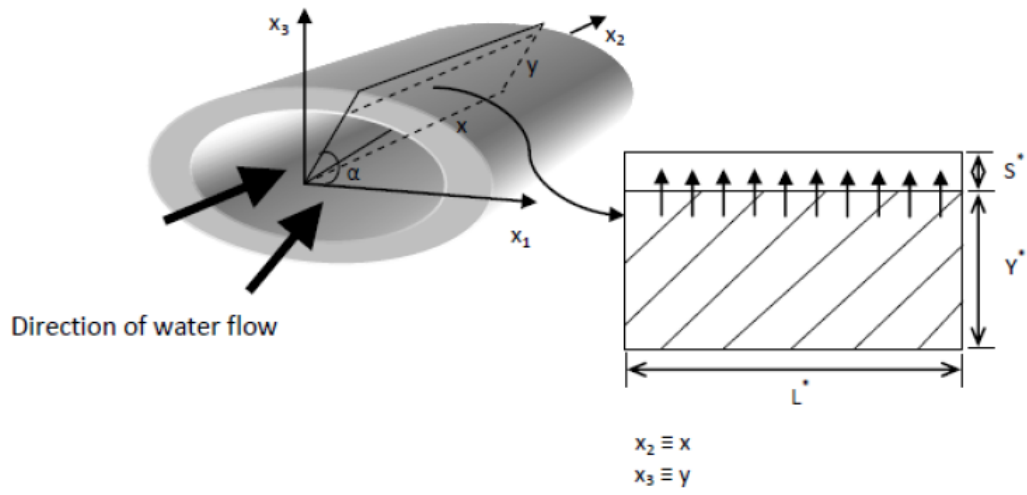


Figure 1: Schematic diagram of the fluid flow

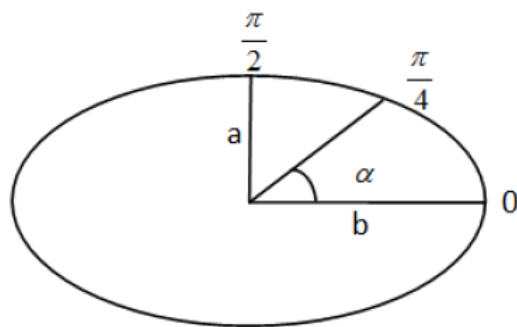


Figure 2: Elliptic cross-section of the pipe

$$\mathbf{U}^* = U_{x_2}^* \mathbf{e}_{x_2} + U_{x_3}^* \mathbf{e}_{x_3}$$

The other unknowns are the pressure p^* in the pipe and p_m^* in the pipe wall. We consider the case for unsteady flow and the governing equations are:

(i) continuity equation (for flow in the pipe)

$$\nabla^* \cdot \mathbf{V}^* = 0 \quad (2.1)$$

(ii) Navier Stokes equation

$$\frac{\partial \mathbf{V}^*}{\partial t^*} + (\mathbf{V}^* \cdot \nabla^*) \mathbf{V}^* = -\frac{1}{\rho^*} \nabla^* p^* + \frac{\mu^*}{\rho^*} \nabla^{*2} \mathbf{V}^* \quad (2.2)$$

(iii) continuity equation (for flow through the pipe wall)

$$\nabla^* \cdot \mathbf{U}^* = 0 \quad (2.3)$$

(iv) Darcy's law

$$\phi \mathbf{U}^* = -\frac{K^*}{\mu^*} \nabla^* p_m^* \quad (2.4)$$

2.1 Dimensionless formulation

The rescaled length components are defined as follows

$$x = \frac{x^*}{L^*}, y = \frac{y^*}{\max(Y^*)}, H = \frac{H^*}{\max(Y^*)}, S = \frac{S^*}{\max(Y^*)}$$

where x and y are normalized length and width, so they vary from zero to unity. The rescaled velocity components are defined as follows

$$V_x = \frac{V_x^*}{V_c^*}, V_y = \frac{V_y^*}{\varepsilon V_c^*}, U_x = \varepsilon \frac{U_x^*}{U_c^*}, U_y = \frac{U_y^*}{U_c^*}$$

where the characteristic velocity U_c^* is taken so that $\phi U_c^* = \varepsilon V_c^*$.

We define the characteristic time as $t_c^* = \frac{L^*}{V_c^*}$.

The inner channel pressure is rescaled by

$$p_c^* = \frac{\mu^* L^* V_c^*}{4Y^{*2}}$$

for laminar flow of a Newtonian fluid, whose viscosity is μ^* with the mean velocity V_c^* .

The fluid characteristic pressure can be defined using equation (2.4), i.e.

$$p_{m,c}^* = \frac{\phi \mu^*}{K^*} S^* U_c^* = \varepsilon \frac{\phi \mu^*}{K^*} S^* V_c^*$$

The ratio between the characteristic wall pressure and the characteristic fluid pressure can be represented as

$$\chi = \frac{p_{m,c}^*}{p_c^*} = \frac{\varepsilon^2 S}{8 Da} \quad (2.5)$$

with $Da = \frac{K^*}{Y^{*2}}$.

2.2 Boundary Conditions

The boundary conditions employed to our fluid flow are;

$$\begin{aligned} p^*(0, y^*, t^*) &= P_{in}^*(t^*) \\ p_m^*(x^*, H^*, t^*) &= 0 \\ p^*(x^*, Y^*, t^*) &= p_m^*(x^*, Y^*, t^*) \\ V_y^*(x^*, Y^*, t^*) &= \phi U_y^*(x^*, Y^*, t^*) \\ V_x^*(x^*, Y^*, t^*) &= 0 \\ V_y^*(x^*, 0, t^*) &= 0 \\ \left. \frac{\partial V_x^*}{\partial y^*} \right|_{y^*=0} &= 0 \end{aligned}$$

The dimensionless boundary conditions are written as follows

$$p|_{x=0} = P_{in}(t) = \frac{P_{in}^*(t)}{p_c^*}, \quad p|_{y=1} = p_m|_{y=1}, \quad p_m|_{y=H} = 0 \quad \frac{\partial p}{\partial x}|_{x=1} = 0 \text{ (dead-end configuration)} \quad (2.6)$$

$$V_y|_{y=1} = U_y|_{y=1}, \quad V_x|_{y=1} = 0, \quad V_x|_{x=1} = 0 \quad (2.7)$$

$$V_y|_{y=0} = 0, \quad \left. \frac{\partial V_x}{\partial y} \right|_{y=0} = 0 \quad (2.8)$$

The Reynolds number is given by

$$Re = \frac{\rho^* V_c^* Y^*}{\mu^*}$$

2.3 Dimensionless system of equations

The continuity equation for the velocity component V_x is defined as

$$\frac{\partial V_x}{\partial x} + \frac{\partial V_y}{\partial y} = 0 \quad (2.9)$$

The equations of motion governing our longitudinal fluid flow can be written as follows

$$\frac{Re}{\varepsilon} \left[\frac{\partial V_x}{\partial t} + V_x \frac{\partial V_x}{\partial x} + V_y \frac{\partial V_x}{\partial y} \right] = -\frac{4}{\varepsilon^2} \frac{\partial p}{\partial x} + \frac{\partial^2 V_x}{\partial x^2} + \frac{1}{\varepsilon^2} \frac{\partial^2 V_x}{\partial y^2} \quad (2.10)$$

$$\frac{Re}{\varepsilon} \left[\frac{\partial V_y}{\partial t} + V_x \frac{\partial V_y}{\partial x} + V_y \frac{\partial V_y}{\partial y} \right] = -\frac{4}{\varepsilon^4} \frac{\partial p}{\partial y} + \frac{\partial^2 V_y}{\partial x^2} + \frac{1}{\varepsilon^2} \frac{\partial^2 V_y}{\partial y^2} \quad (2.11)$$

The equations for flow through the porous walls are governed by the continuity equation and Darcy's Law (2.4) and they are given by

$$\frac{\partial U_x}{\partial x} + \frac{\partial U_y}{\partial y} = 0 \quad (2.12)$$

$$U_x = -\varepsilon^2 \frac{S}{\chi} \frac{\partial p_m}{\partial x} \quad (2.13)$$

$$U_y = -\frac{S}{\chi} \frac{\partial p_m}{\partial y} \quad (2.14)$$

2.4 Homogenization

This method involves writing the governing equations at the pore scale and then introducing an expansion in power series of ε of all the relevant quantities leading to the formulation of the macroscopic governing equations at the various orders in ε [16]. Looking at the small parameter ε , we are interested in the limit problem and its solution when ε tends to zero. With ε small, a regular perturbation expansion for each quantity in the system (2.10 - 2.14) and in the boundary conditions (2.6 - 2.8) can be written as:

$$f(x, y, t) = \sum_{n=0}^{\infty} \overline{f^{(n)}}(x, y, t) \varepsilon^n \quad (2.15)$$

and we match the terms with equal powers. Looking at (2.10) and (2.11) the inertia terms can be neglected at the zero order if the inequality $Re \ll \varepsilon^{-1}$ is satisfied. Since we have assumed that the flow is laminar, then $Re < 1000$. We also assume that the inertial terms are negligible in comparison with the terms having a factor ε^{-k} , with $k \geq 2$ [1].

With the above assumptions, equation (2.11) reduces to

$$\frac{-4}{\varepsilon^4} \frac{\partial p}{\partial y} + \frac{1}{\varepsilon^2} \left(\frac{\partial^2 V_y}{\partial y^2} \right) = 0$$

The term with ε^{-4} approaches zero faster than the term with ε^{-2} . Therefore

$$\frac{-4}{\varepsilon^4} \frac{\partial p}{\partial y} = 0$$

and this yields

$$\frac{\partial p}{\partial y} = 0 \quad (2.16)$$

We immediately deduce that

$$p^{(0)} = p^{(0)}(x, t) \quad (2.17)$$

Now we go to equation (2.10) and this reduces to

$$\begin{aligned} \frac{-4}{\varepsilon^2} \frac{\partial p}{\partial x} + \frac{1}{\varepsilon^2} \frac{\partial^2 V_x}{\partial y^2} &= 0 \\ \frac{\partial^2 V_x}{\partial y^2} &= 4 \frac{\partial p}{\partial x} \\ \frac{\partial V_x}{\partial y} &= 4y \frac{\partial p}{\partial x} + F(x, t) \end{aligned}$$

From the boundary conditions, when $y = 0$ $\frac{\partial V_x}{\partial y} = 0$ and therefore $F(x, t) = 0$.

$$\begin{aligned} \frac{\partial V_x}{\partial y} &= 4y \frac{\partial p}{\partial x} \\ V_x &= 2y^2 \frac{\partial p}{\partial x} + G(x, t) \end{aligned}$$

Next we apply the boundary condition when $y = 1$ and we find that $G(x, t) = -2 \frac{\partial p}{\partial x}$ and this leads to

$$V_x^{(0)}(x, y, t) = 2 \frac{\partial p^{(0)}}{\partial x} (y^2 - 1) \quad (2.18)$$

Looking at the equation for continuity (2.9) we see that $\frac{\partial V_y}{\partial y} = -\frac{\partial V_x}{\partial x}$

Substituting for V_x we get

$$\frac{\partial V_y}{\partial y} = -2 \frac{\partial^2 p^{(0)}}{\partial x^2} (y^2 - 1)$$

Integrating over (0,y) we have

$$\begin{aligned} V_y &= -2 \frac{\partial^2 p^{(0)}}{\partial x^2} \int_0^y (\tau^2 - 1) d\tau \\ &= -2 \frac{\partial^2 p^{(0)}}{\partial x^2} \left[\frac{\tau^3}{3} - \tau \right]_0^y \\ V_y^{(0)}(x, y, t) &= -\frac{\partial^2 p^{(0)}}{\partial x^2} \frac{2y}{3} (y^2 - 3) \end{aligned} \quad (2.19)$$

(2.18) and (2.19) are the equations for velocity within the pipe in the x and y directions respectively

By applying the boundary conditions $V_y|_{y=1} = U_y|_{y=1}$ in (2.19) we obtain

$$U_y^{(0)}(x, 1, t) = \frac{4}{3} \frac{\partial^2 p^{(0)}}{\partial x^2} \quad (2.20)$$

By substituting equations (2.13) and (2.14) in (2.12) we get

$$\begin{aligned} \frac{\partial}{\partial x} \left[-\varepsilon^2 \frac{S}{\chi} \frac{\partial p_m}{\partial x} \right] &= -\frac{\partial}{\partial y} \left[-\frac{S}{\chi} \frac{\partial p_m}{\partial y} \right] \\ -\frac{\varepsilon^2 S}{\chi} \frac{\partial^2 p_m}{\partial x^2} &= -\frac{S}{\chi} \frac{\partial^2 p_m}{\partial y^2} \\ \frac{\partial^2 p_m}{\partial y^2} &= \varepsilon^2 \frac{\partial^2 p_m}{\partial x^2} \end{aligned}$$

According to [11] and [6] the longitudinal pressure gradient is constant. Therefore, from the boundary condition (2.6)₃ $\frac{\partial^2 p_m}{\partial x^2} = 0$ and this implies

$$\begin{aligned} \frac{\partial^2 p_m}{\partial y^2} &= 0 \\ \frac{\partial p_m}{\partial y} &= J(x, t) \\ p_m &= J(x, t)y + K(x, t) \end{aligned} \quad (2.21)$$

By exploiting the boundary conditions (2.6) then $J(x, t) = -\frac{p}{H-1}$ and $K(x, t) = \frac{pH}{H-1}$. Therefore

$$\begin{aligned} p_m &= \left(-\frac{p}{H-1} \right) y + \frac{pH}{H-1} \\ p_m &= p \left(\frac{H-y}{H-1} \right) \\ p_m^{(0)}(x, y, t) &= p^{(0)}(x, t) \left[\frac{H-y}{H-1} \right] \end{aligned} \quad (2.22)$$

We can now write (2.14) as

$$U_y = -\frac{S}{\chi} \frac{\partial p_m}{\partial y} = -\frac{S}{\chi} \left(-\frac{p}{H-1} \right) = \frac{S}{\chi} \left(\frac{p}{H-1} \right) \quad (2.23)$$

and in turn equation (2.20)

$$U_y^{(0)}(x, 1, t) = \frac{4}{3} \frac{\partial^2 p^{(0)}}{\partial x^2} = \frac{S}{\chi} \left(\frac{p^{(0)}}{H-1} \right) \quad (2.24)$$

We now get the equation

$$\frac{\partial^2 p^{(0)}}{\partial x^2} = \frac{3S}{4\chi} \frac{p^{(0)}}{H-1}$$

This is an ordinary differential equation with the boundary conditions (2.6)

$$p^{(0)} = C_1 e^{\sqrt{\frac{3S}{4\chi(H-1)}}x} + C_2 e^{-\sqrt{\frac{3S}{4\chi(H-1)}}x} \quad (2.25)$$

Let $C = \sqrt{\frac{3S}{4\chi(H-1)}}$ Then $p^{(0)} = C_1 e^{Cx} + C_2 e^{-Cx}$

On application of the boundary conditions (2.6) we obtain equations for the constants C_1 and C_2 , that is

$$C_1 = \frac{P_{int}(t)}{1+e^{2C}} \text{ and } C_2 = \frac{P_{int}(t)}{1+e^{-2C}}$$

(2.25) can now be written as

$$p^{(0)} = \frac{P_{in}(t)}{1+e^{2C}} e^{Cx} + \frac{P_{in}(t)}{1+e^{-2C}} e^{-Cx}$$

We can express the pressure profile as follows

$$p^{(0)} = P_{in}(t) \left[\frac{e^{Cx}}{1+e^{2C}} + \frac{e^{-Cx}}{1+e^{-2C}} \right] \quad (2.26)$$

Recalling equations (2.18) and (2.19), we can substitute for $p^{(0)}$ to obtain

$$V_x^{(0)}(x, y, t) = P_{in}(t) 2C \left[\frac{e^{Cx}}{1+e^{2C}} - \frac{e^{-Cx}}{1+e^{-2C}} \right] (y^2 - 1) \quad (2.27)$$

$$V_y^{(0)}(x, y, t) = -P_{in}(t) \frac{2}{3} C^2 \left[\frac{e^{Cx}}{1+e^{2C}} - \frac{e^{-Cx}}{1+e^{-2C}} \right] y(y^2 - 3) \quad (2.28)$$

Equations (2.27) and (2.28) represent the components of the longitudinal velocity in the x and y directions respectively in terms of the pressure.

By squaring C we have $C^2 = \frac{3S}{4\chi(H-1)}$ and we can write (2.24) as

$$U_y^{(0)}(x, 1, t) = \frac{4}{3} C^2 p^{(0)}$$

which on substituting for $p^{(0)}$ yields the equation for velocity through the pores

$$U_y^{(0)}(x, 1, t) = P_{in}(t) \frac{4}{3} C^2 \left[\frac{e^{Cx}}{1+e^{2C}} + \frac{e^{-Cx}}{1+e^{-2C}} \right] \quad (2.29)$$

For the uniform distribution of water along the pipe, we introduce the ratio

$$\begin{aligned}
 \Upsilon = \frac{U_y^{(0)}(1, 1, t)}{U_y^{(0)}(0, 1, t)} &= \frac{P_{in}(t) \frac{4}{3} C^2 \left[\frac{e^C}{1+e^{2C}} + \frac{e^{-C}}{1+e^{-2C}} \right]}{P_{in}(t) \frac{4}{3} C^2 \left[\frac{1}{1+e^{2C}} + \frac{1}{1+e^{-2C}} \right]} \\
 &= \frac{2(e^C + e^{-C})}{e^{-2C} + 2 + e^{2C}} \\
 &= \frac{2(e^C + e^{-C})}{(e^C + e^{-C})^2} \\
 &= \frac{2}{e^C + e^{-C}} \\
 &= \frac{1}{\cosh C} \tag{2.30}
 \end{aligned}$$

and let it be approximately equal to 1. [1].
 We can now make C the subject in (2.30)

$$\begin{aligned}
 C &= \arccos \left[\frac{1}{\Upsilon} \right] \\
 &= \ln \left[\frac{1}{\Upsilon} + \sqrt{\frac{1}{\Upsilon^2} - 1} \right] \\
 &= \ln \left[\frac{1}{\Upsilon} (1 + \sqrt{1 - \Upsilon}) \right] \tag{2.31}
 \end{aligned}$$

with $\Upsilon \leq 1$ and sufficiently close to 1.

By making χ the subject in the equation for C^2 , i.e. $[\chi = \frac{3S}{4C^2(H-1)}]$ we can rewrite the Darcy's equation (2.5) as

$$\begin{aligned}
 Da &= \frac{\varepsilon^2 S}{8\chi} \\
 &= \frac{\varepsilon^2 S}{8 \left[\frac{3S}{4C^2(H-1)} \right]} \\
 &= \frac{\varepsilon^2 C^2 (H-1)}{6} \tag{2.32}
 \end{aligned}$$

We take a value of Υ less than 1, find C and finally obtain the wall permeability K^* .

We still have to find how the inlet pressure $P_{in}^*(t)$ evolves when the reservoir is progressively drained. Let the reservoir be a cylinder of radius R_{res}^* and height h_{res}^* and let h_0^* be the height of its base from the ground. The height $h^*(t^*)$ of the water level within the reservoir will decrease in time and so will the pressure $P_{in}^*(t^*) = \rho^* g^* (h^*(t^*) + h_0^*)$ [1].

Rescaling the heights by h_{res}^* we obtain

$$P_{in}(t) = \frac{\rho^* g^* h_{res}^*}{p_c^*} (h(t) + h_0) \tag{2.33}$$

2.5 Mass flow rate

The equation for mass flow rate for a tube with elliptic cross section can be found in any standard textbook in fluid dynamics (see [17]) yielding;

$$Q = \int_S V(x, y) dS \tag{2.34}$$

Therefore the equations for flow rate at the pipe inlet and outlet through the pores for the elliptic pipe are respectively given by;

$$\begin{aligned}
 Q^*_{in} &= \int_0^1 V_x(0, y, t) dy & (2.35) \\
 &= \int_0^1 2CP_{in}(t) \left[\frac{1}{1+e^{2C}} - \frac{1}{1+e^{-2C}} \right] (y^2 - 1) dy \\
 &= 2CP_{in}(t) \left[\frac{1}{1+e^{2C}} - \frac{1}{1+e^{-2C}} \right] \left[\frac{y^3}{3} - y \right]_0^1 \\
 &= -\frac{4}{3}CP_{in}(t) \left[\frac{1}{1+e^{2C}} - \frac{1}{1+e^{-2C}} \right] \\
 &= -\frac{4}{3}CP_{in}(t) \left[\frac{1+e^{-2C} - (1+e^{2C})}{(1+e^{2C})(1+e^{-2C})} \right] \\
 &= -\frac{4}{3}CP_{in}(t) \left[\frac{e^{-2C} - e^{2C}}{(1+e^{2C})(1+e^{-2C})} \right] \\
 &= \frac{4}{3}CP_{in}(t) \left[\frac{e^{2C} - e^{-2C}}{(1+e^{2C})(1+e^{-2C})} \right] & (2.36)
 \end{aligned}$$

$$\begin{aligned}
 Q^*_{out} &= \int_0^1 U_y(x, 1, t) dx & (2.37) \\
 &= \int_0^1 \frac{4}{3}C^2P_{in}(t) \left[\frac{e^{Cx}}{1+e^{2C}} + \frac{e^{-Cx}}{1+e^{-2C}} \right] dx \\
 &= \frac{4}{3}C^2P_{in}(t) \left[\frac{e^{Cx}}{C(1+e^{2C})} - \frac{e^{-Cx}}{C(1+e^{-2C})} \right]_0^1 \\
 &= \frac{4}{3}CP_{in}(t) \left[\left(\frac{e^C}{1+e^{2C}} - \frac{e^{-C}}{1+e^{-2C}} \right) - \left(\frac{1}{1+e^{2C}} - \frac{1}{1+e^{-2C}} \right) \right] \\
 &= \frac{4}{3}CP_{in}(t) \left[\frac{e^C - 1}{1+e^{2C}} + \frac{1 - e^{-C}}{1+e^{-2C}} \right] \\
 &= \frac{4}{3}CP_{in}(t) \left[\frac{(e^C - 1)(1+e^{-2C}) + (1 - e^{-C})(1+e^{2C})}{(1+e^{2C})(1+e^{-2C})} \right] \\
 &= \frac{4}{3}CP_{in}(t) \left[\frac{e^C + e^{-C} - 1 - e^{-2C} + 1 + e^{2C} - e^{-C} - e^C}{(1+e^{2C})(1+e^{-2C})} \right] \\
 &= \frac{4}{3}CP_{in}(t) \left[\frac{e^{2C} - e^{-2C}}{(1+e^{2C})(1+e^{-2C})} \right] & (2.38)
 \end{aligned}$$

The equation for the mass flow rate is therefore given by $Q^* = \frac{4}{3}CP_{in}(t) \left[\frac{e^{2C} - e^{-2C}}{(1+e^{2C})(1+e^{-2C})} \right]$ and is in terms of pressure and the axial and longitudinal velocities.

3 Results and Discussion

We have considered unsteady fully developed viscous and incompressible flow through an annular pipe with elliptic cross-section. The pipe is made of a flexible and permeable material and this allows water to seep through.

3.1 Pressure profiles

In figure (3) the inlet pressure has been plotted against the length of the pipe, x and it is found to decrease with increase in the length. The fluid pressure has also been plotted against time for different values of x and it is found to decrease with time. It is clear to see that the inlet pressure is equal to the fluid pressure at $x = 0$. There is also a sharp decrease in pressure at the entrance of the pipe but later on the decrease is gradual along the length of the pipe. This is caused by the presence of the pores which is in agreement with the results of [18]. [1] also found that the pressure will decrease in time along the pipe. In addition, from (2.16) the pressure is a function of x only as also shown in figure (3) below.

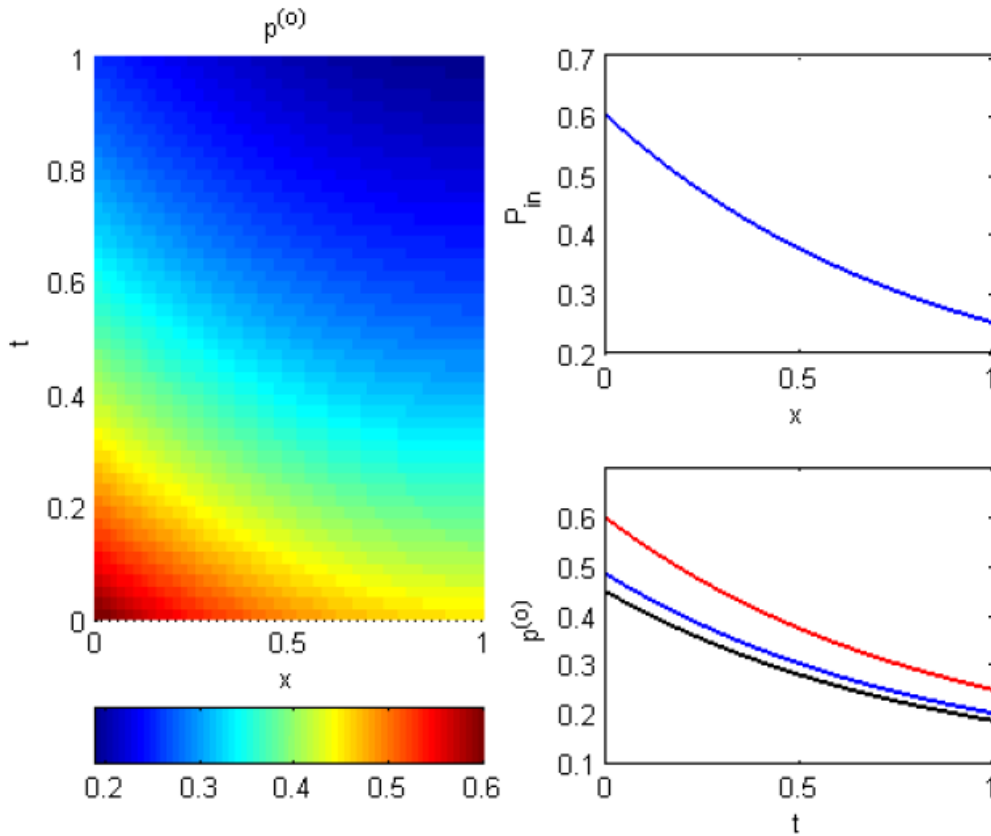


Figure 3: Fluid pressure in pipe and inlet pressure

3.2 Velocity V_x

In figure (4) from the center of the pipe, the velocity tends towards zero along the inner wall of the pipe. Also, from the inlet, the velocity of the fluid tends towards zero along the length of the pipe. The decrease in V_x is attributed to loss of water along the pipe through the pores and also due to the dead end configuration of the pipe. This result is in contrast to that of an elliptic pipe without pores as was studied by [19]. Their results showed that the velocity increased towards the center of the pipe and also increased towards the outlet of the pipe. The velocity does not influence the formation of droplets since it tends to zero at each pore and this is also clear from the boundary conditions (2.7)

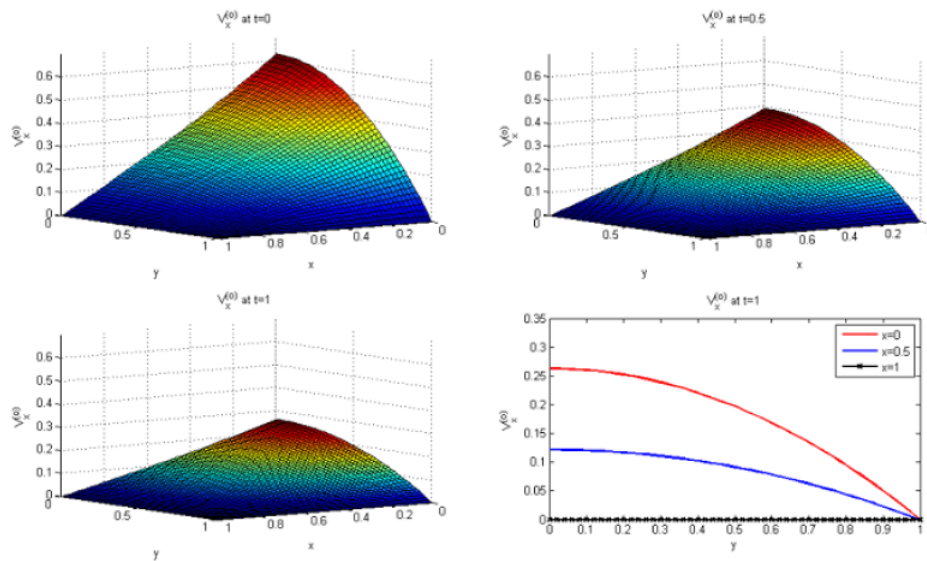


Figure 4: Longitudinal velocity in x direction

3.3 Velocity V_y

In figure (5) the velocity decreases with increase in time. The velocity decreases along the length of the pipe but increases from the center line to the inner wall of the pipe. Initially there is a sharp increase in velocity along y but thereafter the increase is gradual. We can conclude that this increase in V_y from the center line to the wall of the pipe is due to the presence of the pores. This is because [9] studied an elliptical pipe without pores and their result was that the velocity increased from the wall of the pipe towards the center line.

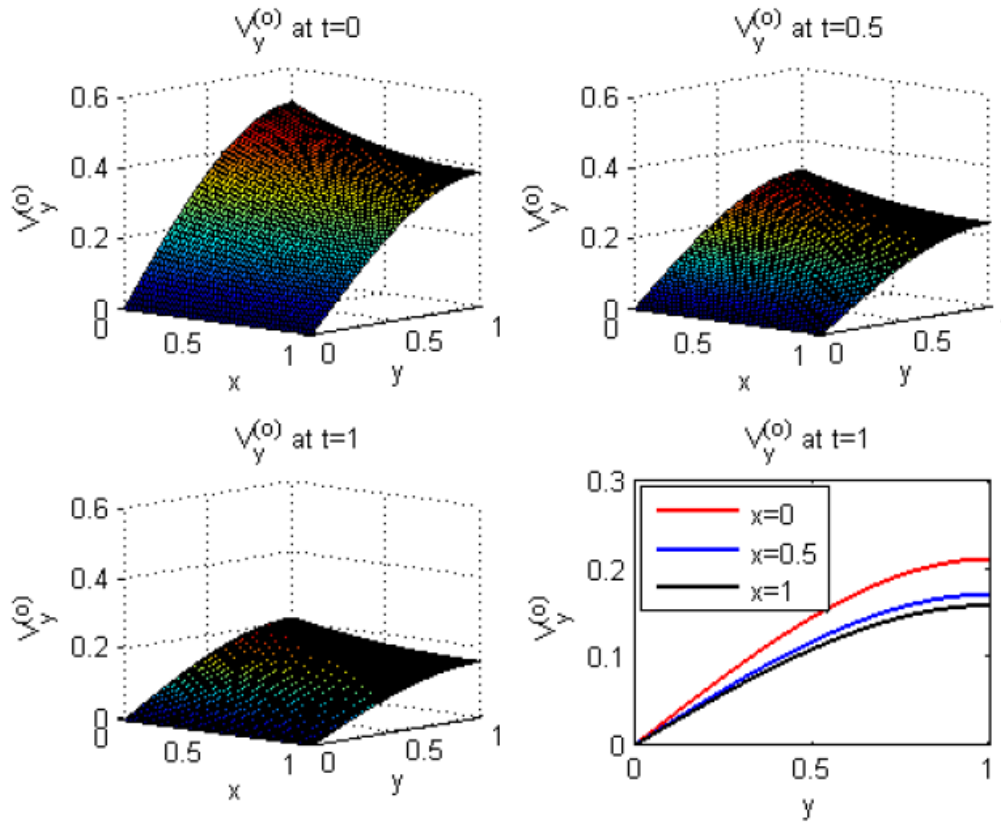


Figure 5: Longitudinal velocity in y direction

3.4 Velocity U_y

In figure (6) the velocity through the pipe outlets decreases along the length of the pipe. In addition, the velocity through the initial outlets increases sharply than through the subsequent outlets. This compares favourably with the study of circular pipes by [20] who found that the tangential velocity component vanishes on the channel wall. In our case the velocity does not vanish but decreases. By rearranging equations (3.7 and 2.5), we find that an increase in the permeability of the pipe leads to an increase in U_y . In this regard, for the velocity through the pipe to be great, we need to increase the permeability of the pipe by adding more pores. Another key observation from the equations is that the thickness of the pipe does not affect the water velocity through the wall. Finally, at each pore, the water velocity through the pipe wall is constant. The explanation for this is in the equation $\frac{\partial p_m}{\partial y} = J(x, t)$ where the pressure gradient across the wall is constant.

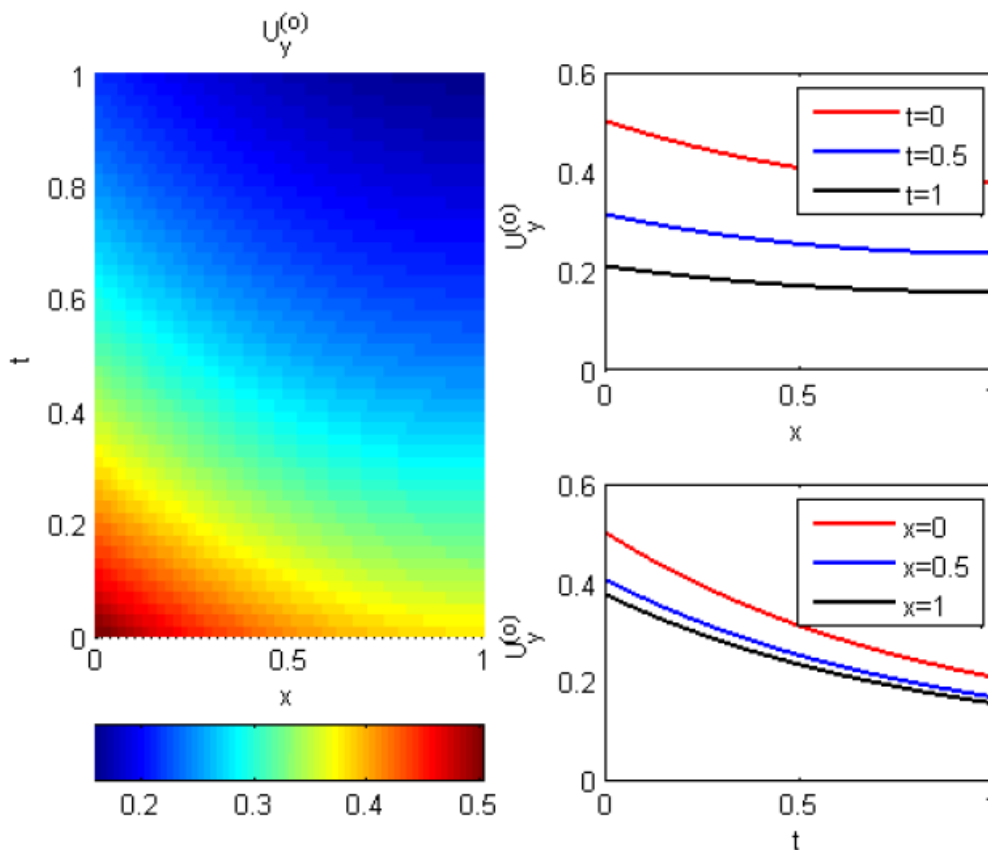


Figure 6: Velocity through the permeable wall

3.5 Mass flow rate

From the mathematical formulation of mass flow rate equation, we find that $Q_{in}^* = Q_{out}^*$ that is, water entering the pipe from the elevated reservoir is equal to the water leaving the pipe through the

pores and therefore the system is operating optimally. The mass flow rate is also directly proportional to the pressure drop and this is in agreement with the work of [9]

Proposition. For efficient use of water for irrigation (through force of gravity) using an annular permeable pipe with elliptic cross section, it is recommended that the pipe be placed in a vertical position.

Proof. In the mathematical formulation of Q_{in}^* and Q_{out}^* above, (2.36 and 2.38) we used $y = 1$ for the boundary conditions and this corresponded to $\alpha = 0$ (see figure 2). Using $y = 0.5$ which corresponds to $\alpha = \frac{\pi}{2}$, the boundary conditions (2.6 and 2.7) will now be;

$$p|_{x=0} = P_{in}(t) = \frac{P_{in}^*(t)}{p_c^*}, \quad p|_{y=0.5} = p_m|_{y=0.5}, \quad p_m|_{y=H} = 0 \quad \frac{\partial p}{\partial x}|_{x=1} = 0 \text{ (dead-end configuration)} \quad (3.1)$$

$$V_y|_{y=0.5} = U_y|_{y=0.5}, \quad V_x|_{y=0.5} = 0, \quad V_x|_{x=1} = 0 \quad (3.2)$$

By applying the boundary conditions (2.8, 3.1 and 3.2) equation (2.18) changes to

$$V_x^{(0)}(x, y, t) = 2 \frac{\partial p^{(0)}}{\partial x} \left(y^2 - \frac{1}{4} \right) \quad (3.3)$$

and (2.19) is now

$$V_y^{(0)}(x, y, t) = - \frac{\partial^2 p^{(0)}}{\partial x^2} \frac{2y}{3} \left(y^2 - \frac{3}{4} \right) \quad (3.4)$$

with (2.20) also changing to

$$U_y^{(0)}(x, 0.5, t) = \frac{1}{6} \frac{\partial^2 p^{(0)}}{\partial x^2} \quad (3.5)$$

Looking at the equation for wall pressure (2.21) and applying the boundary conditions (3.1), then $J(x, t) = -\frac{2p}{2H-1}$ and $K(x, t) = \frac{2pH}{2H-1}$. Therefore equation (2.22) is given by

$$p_m^{(0)}(x, y, t) = 2p^{(0)}(x, t) \left[\frac{H-y}{2H-1} \right] \quad (3.6)$$

We can now write (2.14) as

$$U_y = -\frac{S}{\chi} \frac{\partial p_m}{\partial y} = -\frac{S}{\chi} \left(-\frac{2p}{2H-1} \right) = \frac{S}{\chi} \left(\frac{2p}{2H-1} \right) \quad (3.7)$$

and in turn equation (3.5)

$$U_y^{(0)}(x, 0.5, t) = \frac{1}{6} \frac{\partial^2 p^{(0)}}{\partial x^2} = \frac{S}{\chi} \left(\frac{2p^{(0)}}{2H-1} \right)$$

We now get the equation

$$\frac{\partial^2 p^{(0)}}{\partial x^2} = \frac{6S}{\chi} \frac{2p^{(0)}}{2H-1}$$

This is an ordinary differential equation with the boundary conditions (3.1)

$$p^{(0)} = C_1 e^{\sqrt{\frac{12S}{\chi(2H-1)}} x} + C_2 e^{-\sqrt{\frac{12S}{\chi(2H-1)}} x} \quad (3.8)$$

Let $C = \sqrt{\frac{12S}{\chi(2H-1)}}$ Then $p^{(0)} = C_1 e^{Cx} + C_2 e^{-Cx}$

By substituting the equation for pressure (2.26) in the equations (3.3, 3.4 and 3.5) we get the equations for the velocities in terms of pressure and they are respectively as follows

$$V_x^{(0)}(x, y, t) = P_{in}(t)2C \left[\frac{e^{Cx}}{1 + e^{2C}} - \frac{e^{-Cx}}{1 + e^{-2C}} \right] \left(y^2 - \frac{1}{4} \right) \quad (3.9)$$

$$V_y^{(0)}(x, y, t) = -P_{in}(t) \frac{2}{3} C^2 \left[\frac{e^{Cx}}{1 + e^{2C}} - \frac{e^{-Cx}}{1 + e^{-2C}} \right] y \left(y^2 - \frac{3}{4} \right) \quad (3.10)$$

$$U_y^{(0)}(x, y, t) = P_{in}(t) \frac{1}{6} C^2 \left[\frac{e^{Cx}}{1 + e^{2C}} + \frac{e^{-Cx}}{1 + e^{-2C}} \right] \quad (3.11)$$

Next we look at the equations for the mass flow rate (2.36 and 2.37) and these will change to

$$Q^*_{in} = \int_0^{0.5} V_x(0, y, t) dy = \frac{1}{6} CP_{in}(t) \left[\frac{e^{2C} - e^{-2C}}{(1 + e^{2C})(1 + e^{-2C})} \right] \quad (3.12)$$

and

$$Q^*_{out} = \int_0^1 U_y(x, 0.5, t) dx = \frac{1}{6} CP_{in}(t) \left[\frac{e^{2C} - e^{-2C}}{(1 + e^{2C})(1 + e^{-2C})} \right] \quad (3.13)$$

respectively

Subsequently, for $y = 0.75$ corresponding to $\alpha = \frac{\pi}{4}$, the equation for the mass flow rate is:

$$Q^*_{in} = Q^*_{out} = \frac{9}{16} CP_{in}(t) \left[\frac{e^{2C} - e^{-2C}}{(1 + e^{2C})(1 + e^{-2C})} \right] \quad (3.14)$$

Thus looking at the above equations the mass flow rate is maximum when $\alpha = 0$ and this lies on the major axis of the ellipse and is minimum when $\alpha = \frac{\pi}{2}$ which is on the minor axis. Therefore for the efficient use of water for irrigation, the permeable elliptical pipe should be laid in a vertical position as shown in figure (7)

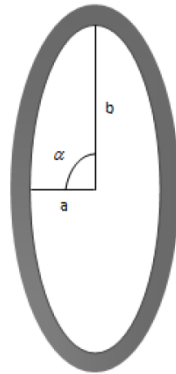


Figure 7: Vertical elliptical cross section

Hence the proof. □

4 Conclusion

In this work, the homogenization method was used to study the flow of incompressible fully developed flow in a horizontal pipe of elliptical cross-section. The advantage of this method is that the equations

are derived from the fundamental laws of fluid dynamics rather than heuristic assumptions and therefore they have a sound physical basis. It also averages values of the dependent variables over large scales and renders a good approximation of the fine scale solution. The following points summarize the principal results of this study:

- (i) The mass flow rate was shown to be maximum along the major axis meaning that the elliptical pipe should be placed in a vertical position for efficient usage of water for irrigation.
- (ii) The velocity through the pipe wall is not affected by the thickness of the pipe and at each pore the velocity is uniform and constant. Indeed the formation of droplets at each pore for irrigation is uniform along the pipe.
- (iii) The presence of pores leads to an increase in velocity from the center line towards the wall of the pipe. This proposed solution can be directly used for computing wall shear stress distribution along the boundary of the wall.

Acknowledgment

The results presented in this paper were obtained in the course of Doctoral studies for the corresponding author sponsored by The German Academic Exchange Service (DAAD). The authors gratefully acknowledge the financial support of DAAD.

Authors Contributions

The authors have developed all the main sections of the paper jointly. The analytical solutions have been produced by all the authors while the programming and related plots have been produced by M.M. All authors read and approved the final manuscript.

Competing Interests

The authors declare that no competing interests exist.

References

- [1] Fasano A, Farina A. Designing irrigation pipes. *Journal of Mathematics in Industry*. 2011;1:8.
- [2] Akbari M, Sinton D, Bahrami M. Viscous flow in variable cross-section microchannels of arbitrary shapes. *International Journal of Heat and Mass Transfer*. 2011;54:3970-3978.
- [3] Akbari M, Tamayol A, Bahrami M. A General Model for Predicting low Reynolds number flow pressure drop in non-uniform microchannels of non-circular cross section in continuum and slip flow regimes. *J. Fl. Eng*. 2013;135(7):071205.
- [4] Tamayol A, Bahrami M. Direct numerical simulation of the turbulent flow in an elliptical pipe. *Computational Mathematics and Mathematical Physics*. 2010;46(8):1453-1461.
- [5] Adachi T. Linear stability of flow in rectangular ducts in the vicinity of the critical aspect ratio. *Eur. J. of Mech. - B/Fl*. 2013;41:163-168.

- [6] Islam S, Bano Z, Haroon T, Siddiqui AM. Unsteady poiseuille flow of second grade fluid in a tube of elliptical cross section. In: Proceedings of the Romanian Academy, Series A, Italy. 2011;12(4):291-295.
- [7] Dos Santos RG, Figueiredo JR. Laminar elliptic flow in the entrance region of tubes. J. Braz. Soc. Mech. Sci. and Eng. 2007;29(3):233.
- [8] Voronova TV, Nikitin NV. Direct numerical simulation of the turbulent flow in an elliptical pipe. Computational Mathematics and Mathematical Physics. 2006;46(8):1453-1461.
- [9] Cade MA, Lima WCPB, Neto SR, Lima AGB. Natural gas laminar flow in elliptic cylindrical pipes: A numerical study. Brazilian Journal of Petroleum and Gas. 2010;4(1):019-033.
- [10] Graur I, Sharipov F. Gas flow through an elliptical tube over the whole range of the gas rarefaction. European Journal of Mechanics B/Fluids. 2008;27:335-345.
- [11] Lekner J. Flow with slip between coaxial cylinders and in an equilateral triangular pipe. The Open Appl. Phys. J. 2009;2:27-31.
- [12] Rykov VA, Titarev VA, Shakhov EM. Rarefied poiseuille flow in elliptical and rectangular tubes. Fluid Dynamics. 2011;46(3):456-466.
- [13] Timofte C. Upscaling in diffusion problems in domains with semipermeable boundaries. Acta Physica Polonica B. 2007;38(8):2433-2443.
- [14] Dagan G, Fiori A, Jankovic I. Upscaling of heterogeneous porous formations: Critical examination and issues of principle. Adv. in Wat. Res. 2013;51: 67-85.
- [15] Orgeas L, Geindreau C, Auriault JL, Bloch JF. Upscaling the flow of generalised Newtonian fluids through anisotropic porous media. J. Non-Newtonian Fluid Mech. 2007;145:15-29.
- [16] Fasano A, Farina A. Modelling complex flows in porous media by means of upscaling procedures. Rend. Istit. Mat. Univ. Trieste. 2010;42:65-102.
- [17] Chorlton F. Textbook of Fluid Dynamics. India: CBS Publishers and Distributors 1985:335.
- [18] Nebbali R, Bouhaded K. Non-newtonian fluid flow in plane channels: Heat transfer enhancement using porous blocks. Int. J. of Therm. Sci. 2011;50(10):1984-1995.
- [19] Lasode OA, Papoola OT, Prasad BVSS. Pressure drop in liquefied petroleum gas laminar flow in cylindrical elliptic pipes. Braz. J. of Pet. and Gas. 2013;7(4):169-179.
- [20] Jensen KH. Slow flow in channels with porous walls; 2012. ; <http://arxiv:1208.5423> [physics.flu-dyn]

©2015 Ndegwa et al.; This is an Open Access article distributed under the terms of the Creative Commons Attribution License <http://creativecommons.org/licenses/by/4.0>, which permits unrestricted use, distribution, and reproduction in any medium, provided the original work is properly cited.

Peer-review history:

The peer review history for this paper can be accessed here (Please copy paste the total link in your browser address bar)

www.sciencedomain.org/review-history.php?iid=726&id=6&aid=6661